Magnetic hyperfine interaction in $CeMn_2Ge_2$ and $CeMn_2Si_2$ measured by perturbed angular correlation spectroscopy

A. W. Carbonari,* J. Mestnik-Filho, R. N. Saxena, and M. V. Lalić†
Instituto de Pesquisas Energéticas e Nucleares-IPEN-CNEN/SP, P.O. Box 11049, 05422-970 São Paulo, São Paulo, Brazil
(Received 14 May 2003; revised manuscript received 19 August 2003; published 26 April 2004)

Time differential perturbed γ-γ angular correlation technique has been used to measure the magnetic hyperfine field at both Mn and Ce atom sites in $CeMn_2Ge_2$ and $CeMn_2Si_2$ intermetallic compounds. The probe nucleus $^{111}In \rightarrow {}^{111}Cd$ was used to investigate the hyperfine interaction at Mn sites, while the $^{140}La \rightarrow {}^{140}Ce$ was used to measure the magnetic hyperfine field at Ce. Present measurements cover the temperature range from 10 to 460 K in both compounds. Measurements with ^{111}Cd probe show pure electric quadrupole interactions above 420 K in both compounds and a combined magnetic dipole and electric quadrupole interaction below respective magnetic transition temperatures. While the temperature dependence of the hyperfine field at ^{111}Cd on Mn site in the $CeMn_2Si_2$ showed a standard behavior for an antiferromagnetic compound below $T_N \approx 408$ K, the temperature dependence of magnetic hyperline field (MHF) in $CeMn_2Ge_2$ showed a transition from ferromagnetic to antiferromagnetic phase at around 320 K and from antiferromagnetic to paramagnetic phase at 420 K. No hyperfine field was observed at ^{140}Ce in $CeMn_2Si_2$ in the temperature range from 10 K to 400 K. A unique and well-defined magnetic interaction is observed at Ce sites in $CeMn_2Ge_2$ below 320 K, corresponding to a ferromagnetic ordering of Mn moments. The temperature dependence of MHF, however, shows a sharp deviation from an expected Brillouin-like behavior for temperatures below 120 K. The additional magnetic interaction is believed to result from the polarization of Ce spin moments induced by the magnetic field from Mn moments.

DOI: 10.1103/PhysRevB.69.144425 PACS number(s): 76.80.+y, 75.20.Hr, 31.30.Gs

I. INTRODUCTION

Intermetallic compounds of the type RT_2X_2, where R is a rare-earth or actinide ion, T is a transition metal, and X is an sp element such as Si, Ge, Sn, or Sb, form a large family, which exhibits very interesting physical phenomena. In particular, the compounds where $R=$Ce and $X=$Si or Ge have been studied quite intensively since the discovery[1] of superconductivity in the heavy fermion $CeCu_2Si_2$, and have shown a rich variety of different properties such as magnetism, superconductivity, mixed valence, heavy fermion, or Kondo behavior. Among these compounds, those with $T=$Mn are reported[2,3] to have a special feature: they are the only members of the family, which exhibit magnetic moments exclusively at Mn. A detailed investigation of these compounds can, therefore, be very useful in the effort to understand the complex behavior of the RT_2X_2 series and the origin of their magnetic interactions.

The $CeMn_2X_2$ ($X=$Si,Ge) compounds crystallize in a body-centered tetragonal $ThCr_2Si_2$-type (space group $I4/mmm$) structure in which the Ce atoms occupy $2a$ (0,0,0) positions, the Mn atoms occupy $4d$ (0,1/2,1/4) positions forming a simple tetragonal sublattice, and the X atoms occupy $4e$ (0,0,z) positions. Therefore, the crystal structure is formed by stacked atomic layers along the c axis with the Mn-X-Ce-X-Mn sequence of atomic planes.

Nowik *et al.*[4] observed from the Mössbauer spectroscopy measurements that $CeMn_2Ge_2$ has an antiferromagnetic ordering with a Néel temperature of $T_N=390$ K. In a later work, Fernandez-Baca *et al.*,[5] using neutron-diffraction measurements, concluded that $CeMn_2Ge_2$ shows a collinear commensurate antiferromagnetic phase below $T_N \approx 415$ K. It has also been reported[5,6] that at the Curie temperature $T_C \approx 320$ K, there is a transition to an incommensurate ferromagnetic component of the Mn moments in the c axis and a helical component in the ab plane. The compound $CeMn_2Si_2$ has a collinear antiferromagnetic order below 380 K.[3,5] In $CeMn_2Si_2$ the magnetic structure is such that the intralayer exchange interaction between Mn moments is ferromagnetic, and the interlayer is antiferromagnetic. For $CeMn_2Ge_2$, below Néel temperature, the intralayer exchange is antiferromagnetic and undergoes a transition to an incommensurate conical structure in the ferromagnetic phase. There are significant differences in the magnetic-moment values, reported in the literature, for both compounds.[3,5]

Although the magnetic phase-transition behavior of the $CeMn_2Ge_2$ and $CeMn_2Si_2$ compounds has been studied by other techniques,[3,5,6] only one microscopic study[4] on atomic scale has been reported. In the present work, the magnetic dipole and electric quadrupole interactions, at the Ce and Mn sites, were investigated by the time differential perturbed γ-γ angular correlation (TDPAC) spectroscopy. This method requires only a small amount of radioactive probe nuclei (tracers in most cases) and offers a high sensitivity to local distance variations in the crystal lattice and, consequently, can be used to follow changes such as magnetic ordering, bond distances, symmetry, defect trapping, etc. on a microscopic scale by measuring the electric-field gradient (EFG) and magnetic hyperfine field (MHF) at probe sites. TDPAC is also the only technique, among all the radioactive hyperfine methods, that uses the ^{140}Ce as probe nuclei, which in the present case is crucial for investigating the local magnetic behavior of Ce atoms. The investigation of the MHF at Ce atoms in $CeMn_2Ge_2$ and $CeMn_2Si_2$ is quite important to

clarify as to why these compounds do not really present magnetic ordering at Ce sites, or if there exists some magnetic polarization of the Ce electrons which is not seen by macroscopic techniques. TDPAC measurements were performed in $CeMn_2Ge_2$ and $CeMn_2Si_2$ compounds as a function of temperature, using $^{111}In \rightarrow {}^{111}Cd$ probe to obtain information about microscopic details of their electronic and magnetic structures and the temperature dependence of the EFG and MHF at Mn sites. Some of the PAC data for $CeMn_2Ge_2$ using ^{111}Cd probe were already presented in an earlier publication.[7] In the present work we have extended the analysis of these data to further investigate the temperature dependence of the EFG and its relation with the magnetic behavior. Moreover, we present and discuss the results of the MHF values for both $CeMn_2Ge_2$ and $CeMn_2Si_2$ compounds. Additional measurements were carried out below Néel temperature of both compounds using $^{140}La \rightarrow {}^{140}Ce$ probe to investigate the local magnetic field at Ce sites.

II. EXPERIMENTAL PROCEDURE

Stoichiometric polycrystalline samples of $CeMn_2Ge_2$ and $CeMn_2Si_2$ were prepared by repeatedly melting the constituent elements (Ce 99.99%, Mn 99.9985%, Ge 99.9995%) along with the radioactive tracers under argon atmosphere purified with a hot titanium getterer. Radioactive probe nuclei used were carrier free ^{111}In purchased from MDS Nordion, and ^{140}La obtained by neutron irradiation of lanthanum metal in the IEA-R1 research reactor at IPEN that substitutes for less than 0.1% of Ce atoms. The samples were annealed under an atmosphere of ultrapure Ar for 48 h at 700 °C.

The hyperfine interaction of the 245 keV, $5/2^+$ spin state of ^{111}Cd probe nuclei in the polycrystalline samples of $CeMn_2Ge_2$ and $CeMn_2Si_2$ was measured by the TDPAC technique utilizing the (171–245) keV γ-γ cascade. The γ-γ cascade of (329–487) keV populated from the β decay of ^{140}La was used for the measurement of magnetic interaction of the 2083 keV, 4^+ spin state in ^{140}Ce. TDPAC spectra were recorded at several temperatures using a standard setup with four BaF_2 detectors arranged in a planar 90°–180° geometry, generating simultaneously 12 delayed coincidence spectra. The detector system had a time resolution of 600 ps. For low-temperature measurements the sample was attached to the cold finger of a closed-cycle-helium refrigerator with temperature controlled to better than 0.1 K. Spin rotation spectra $R(t)$ were generated from the background subtracted coincidence counts $C(\theta,t)$:

$$R(t) = 2\left[\frac{C(180°,t) - C(90°,t)}{C(180°,t) + 2C(90°,t)}\right], \tag{1}$$

where $C(\theta,t)$ are the geometric mean of the coincidences taken from the spectra recorded at angle θ. Above the magnetic transition temperature, the measured perturbation function $R(t)$ was fitted to the following expression for the static electric quadrupole interaction:

$$R(t) = A_{22}G_{22}(t) = A_{22}\sum_i f_i G_{22}^i(t), \tag{2}$$

where A_{22} is the unperturbed angular correlation coefficient, f_i are the fractional site populations, and $G_{22}^i(t)$ are the corresponding perturbation factors given by

$$G_{22}(t) = S_{20} + \sum_{n=1}^{3} S_{2n}\cos(\omega_n t)\exp(-\omega_n^2\tau_R^2/2) \times \exp(-\omega_n^2\delta^2 t^2/2), \tag{3}$$

The primary frequencies ω_n and their amplitudes S_{2n} are related to the hyperfine splitting of the intermediate nuclear level and depend on the nuclear quadrupole frequency $\omega_Q = eQV_{zz}/4I(2I-1)\hbar$ and the asymmetry parameter $\eta = (V_{xx} - V_{yy})/V_{zz}$, where V_{xx}, V_{yy}, and V_{zz} are the elements of the EFG tensor in its principal axis system. Generally one uses the spin independent quadrupole frequency defined by $\nu_Q = eQV_{zz}/h$, where Q is the nuclear electric quadrupole moment of the intermediate level. The known quadrupole moment of 0.83 b for the $I = 5/2^+$ intermediate level of ^{111}Cd has been used to determine V_{zz}. The effect of finite time resolution τ_R of detectors and the distribution of EFG with a relative width δ are properly taken into account in Eq. (3).

In order to fit the perturbation functions measured at temperatures below T_C or T_N, we used a model which included combined electric and magnetic interaction in a polycrystalline sample from which the quadrupole frequency ν_Q as well as the Larmor frequency $\omega_L = g\mu_N B_{hf}/\hbar$, where g is the nuclear g factor and B_{hf} is magnetic hyperfine field, can be deduced. The known values of the g factors, $g = 0.306$ and $g = 1.12$ for the $I = 5/2^+$ and the $I = 4^+$ intermediate levels of ^{111}Cd and ^{140}Ce, respectively, were used to determine the corresponding magnetic hyperfine field B_{hf}.

III. EXPERIMENTAL RESULTS

Crystal structures of the samples were checked by powder x-ray-diffraction measurements at room temperature. The results confirmed a predominant phase, with $ThCr_2Si_2$ prototype structure, in both compounds. The magnetization measurements were carried out by a super conducting quantum interference device magnetometer and the results confirmed the antiferromagnetic phase with Néel temperature of $\sim$380 K for $CeMn_2Si_2$ and the ferromagnetic phase with $T_C \approx 320$ K for $CeMn_2Ge_2$.

Some of the perturbation functions, measured in the temperature range from 15 to 460 K using ^{111}Cd probe, are shown in Fig. 1 for $CeMn_2Si_2$ samples along with their Fourier transforms. In the case of $CeMn_2Ge_2$ the perturbed angular correlation (PAC) spectra above T_C were least-squares fitted with two-probe site model using theoretical perturbation function given by Eq. (3). The Fourier spectrum shows two fractions with sharp ($\delta < 1\%$) and well-resolved frequencies. The major fraction ($\sim$75%) is axially symmetric ($\eta = 0$) with a very small value of the quadrupole frequency $\nu_Q = 3.5$ MHz while the other fraction is characterized by a quadrupole frequency $\nu_Q = 121$ MHz and $\eta \approx 0.37$. In the case of $CeMn_2Si_2$ the spectra above T_N could also be fitted with two probe sites but showed a wider frequency distribu-

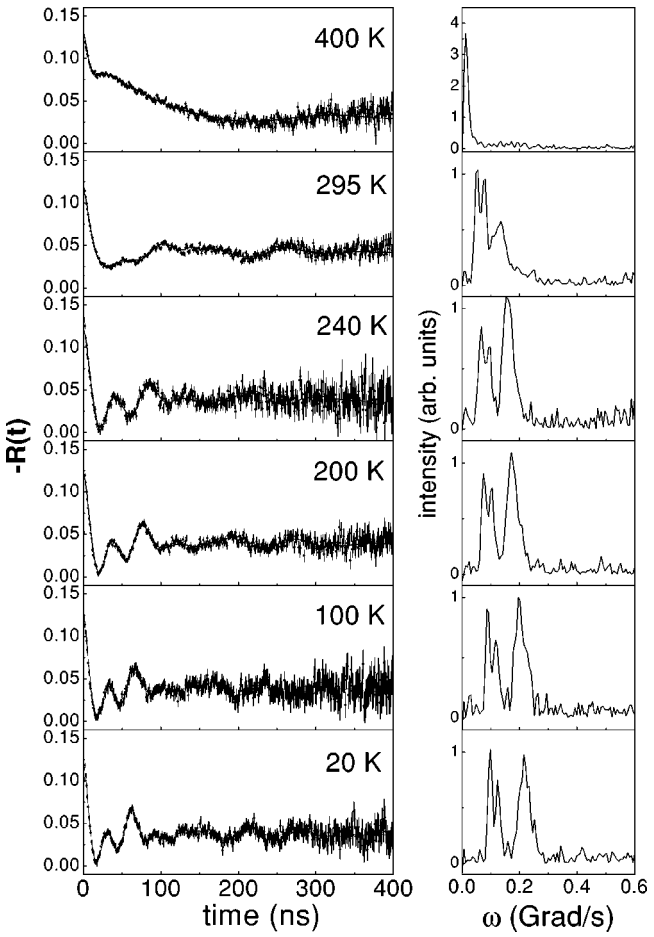

FIG. 1. The perturbation functions and their Fourier transforms for ^{111}Cd probes in $CeMn_2Si_2$ compound at various temperatures. Solid lines are the least-squares fits of the theoretical function to the experimental data.

tion. The major fraction ($\sim$60%) in this case corresponds to the higher quadrupole frequency $\nu_Q = 110$ MHz with $\eta \approx 0.50$ and $\delta \approx 35\%$, while the smaller fraction corresponds to $\nu_Q \approx 8$ MHz with $\eta = 0$ and $\delta \approx 5\%$. In both compounds, we have associated the lower frequencies to the ^{111}Cd probe substituting the Mn atoms and the higher frequency to the probe substituting either Ce or Ge(Si)atoms. These assignments are consistent with an *ab initio* calculation using full-potential–linear augmented plane wave (FP-LAPW) method.[8] Calculated values of EFG at Mn in both compounds are much smaller compared to those at Ce or Ge(Si).

The assignments are also consistent with the results of magnetic hyperfine field in these compounds which are discussed below. The calculated values of EFG at Ce and Ge(Si) atoms, however, do not give any clue about the higher frequencies as to whether they correspond to Ce or Ge(Si) sites. Since only very weak or no magnetic interactions were observed for these fractions, we shall focus our attention on the fractions which correspond to the Mn sites in both compounds.

Below respective magnetic transition temperatures, PAC spectra for both compounds were fitted with a model which accounts for the combined electric quadrupole and magnetic

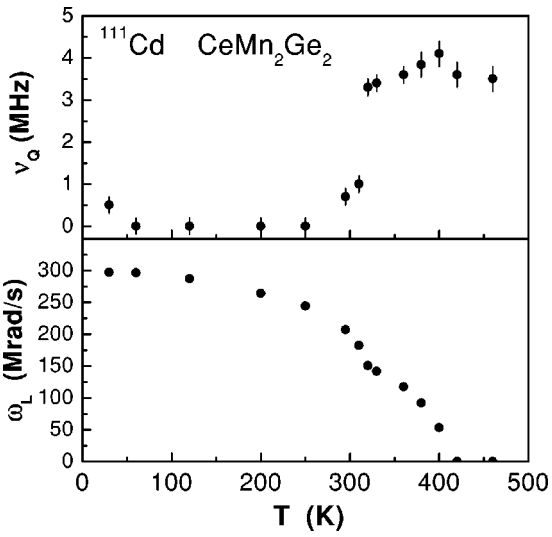

FIG. 2. The temperature dependence of fitted quadrupole frequency ν_Q (top) and Larmor frequency ω_L (bottom) for ^{111}Cd at Mn sites in $CeMn_2Ge_2$.

dipole interactions. The Larmor frequency ω_L as well as the quadrupole frequency ν_Q for the major fraction, measured for ^{111}Cd in $CeMn_2Ge_2$, is plotted as a function of temperature in Fig. 2. A change in the slope of the curve around 320 K is clearly seen. The same effect is observed with Mössbauer studies,[4] and reflects the transition from an antiferromagnetic to ferromagnetic order at this temperature. For temperatures below 320 K, in the ferromagnetic phase, the values of Larmor frequency follow a normal Brillouin curve. It was demonstrated from the Mössbauer studies that the doped ^{57}Fe occupies mainly the Mn site in $CeMn_2Ge_2$. Since we observed a remarkable similarity between the temperature dependence of the hyperfine field as well as the EFG in the present PAC experiment with the earlier Mössbauer experiment,[4] we also conclude that the major fraction of ^{111}Cd probes indeed replace the Mn atoms in this compound.

At 15 K, where the curve reaches the saturation region, the measured values of ω_L and the corresponding hyperfine field B_{hf} are, respectively, 297.1(3) Mrad/s and 20.3(1) T. The hyperfine fields as well as the largest component of the EFG tensor V_{zz}, are in the direction of the *c* axis. Temperature dependence of the Larmor frequency measured for the ^{111}Cd probe substituting for Mn sites in $CeMn_2Si_2$ is shown in Fig. 3.

The measured Larmor frequency of 101.8(3) Mrad/s at 20 K gives $B_{hf} = 6.96(2)$ T. Just below the magnetic transition temperature, in the critical region for both compounds, we considered the first five points to fit the experimental ω_L values to the well-known power-law $\omega_L(T) = \omega_L(0)(1 - T/T_N)^{\beta}$ for magnetic materials. The resulting parameters are $\omega_L(0) = 283(8)$ Mrad/s, $B_{hf}(0) = 19.3(5)$ T, exponent $\beta = 0.41(2)$, and $T_N = 408(2)$ for $CeMn_2Ge_2$ and $\omega_L(0) = 112(5)$ Mrad/s, $B_{hf}(0) = 7.7(4)$ T, exponent $\beta = 0.43(3)$ and $T_N = 379(4)$ for $CeMn_2Si_2$. The values of Néel temperatures obtained here agree quite well with those obtained by neutron-diffraction measurements.[3,5]

Some of the PAC spectra for $CeMn_2Ge_2$ and $CeMn_2Si_2$,

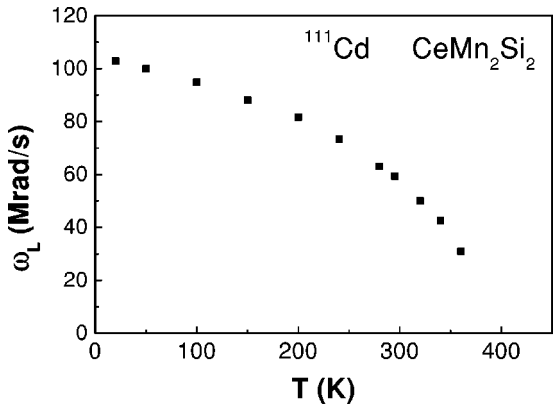

FIG. 3. The temperature dependence of fitted Larmor frequency (ω_L) for ^{111}Cd at Mn sites in $CeMn_2Si_2$.

measured by using the $^{140}La \rightarrow {}^{140}Ce$ probe, obtained just above and below respective Néel temperatures are shown in Fig. 4 and Fig. 5, respectively.

As the quadrupole moment of the 2083 keV 4^+ state of

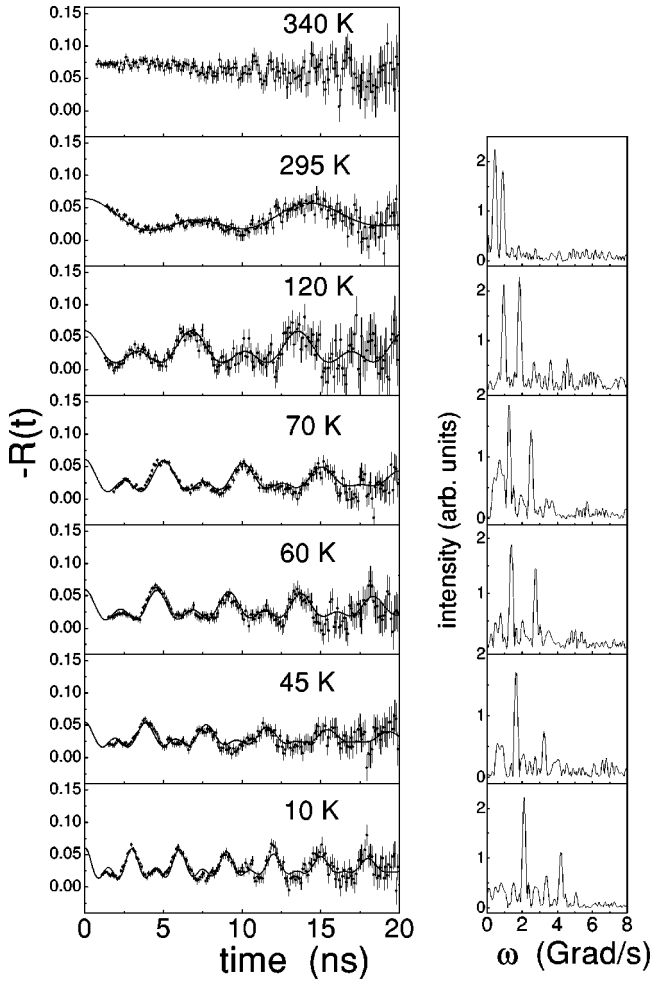

FIG. 4. The perturbation functions $R(t)$ and their Fourier transforms for ^{140}Ce probes in $CeMn_2Ge_2$ compound at various temperatures. Solid lines are the least-squares fits of the theoretical function to the experimental data.

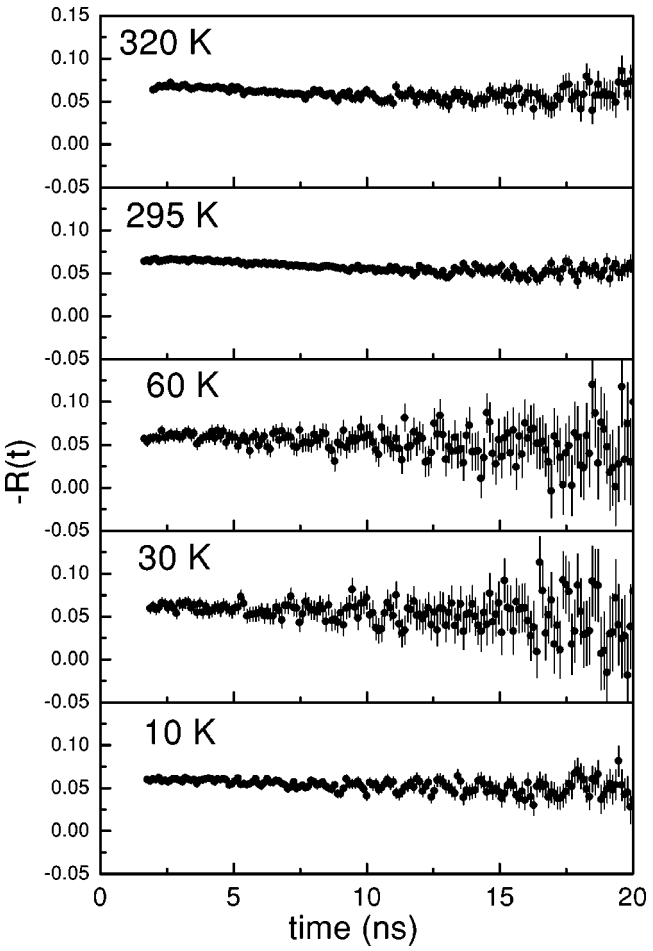

FIG. 5. Perturbation functions $R(t)$ for ^{140}Ce probes in $CeMn_2Si_2$ compound at some temperatures.

^{140}Ce is known to be very small,[9] one expects to observe an almost pure magnetic dipole interaction, at the Ce site, below Néel temperatures. Since the probe ^{140}Ce is not an impurity atom in $CeMn_2Ge_2$ and $CeMn_2Si_2$ compounds, its use in PAC experiments is unique among the microscopic methods.

No hyperfine field was observed in $CeMn_2Si_2$ in the temperature range from 10 K to 400 K and in $CeMn_2Ge_2$ between 410 K and 320 K. This is consistent with the symmetry considerations of the spin-''up'' and spin-''down'' arrangement of the Mn superlattice around the Ce site in the antiferromagnetic phases in both compounds. Below 320 K, a unique and well-resolved magnetic interaction is observed at Ce in $CeMn_2Ge_2$. The temperature dependence of the Larmor frequency ω_L is plotted in Fig. 6. The observed magnetic interaction corresponds to the ferromagnetic ordering of the Mn moments.

The measurements below 150 K, however, show a sharp deviation from an expected Brillouin-like behavior for a simple ferromagnetic ordering. The Ce hyperfine field, instead of approaching a saturation value, increases sharply at lower temperatures. The measured hyperfine field at 150 K is 15.9(4) T while at 10 K it is 39.04(7) T. This result contrasts the regular temperature dependence of the hyperfine field at Mn site measured by the ^{111}Cd probe Fig. 2, as well as the

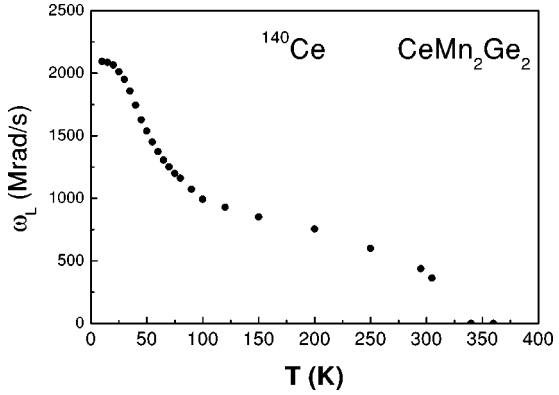

FIG. 6. The temperature dependence of fitted Larmor frequency (ω_L) for ^{140}Ce at Ce sites in $CeMn_2Ge_2$ compound.

results of the magnetization measurement in $CeMn_2Ge_2$. The results clearly indicate that below 150 K there is an additional contribution to the MHF, most probably from the polarization of the Ce spins in the compound. The estimated Ce contribution to the MHF at 0 K corresponds roughly to $\sim$20 T. This is just about half the value found for the MHF at Ce site, extrapolated to 0 K, in the $CeIn_3$ intermetallic compound.[10] $CeIn_3$ is a concentrated Kondo system where the Ce moments order antiferromagnetically and, therefore, expected to present smaller MHF values than those presented by ferromagnetically ordered Ce system. The fact that the Ce spin contribution to the MHF at Ce site in $CeMn_2Ge_2$ is much smaller indicates a weaker Ce spin alignment mechanism in this compound.

IV. DISCUSSION

Neutron-diffraction measurements[3,5,6] have determined the magnetic structure of $CeMn_2Si_2$ and $CeMn_2Ge_2$. The former has a collinear antiferromagnetic structure where all the manganese moments within the same plane (intralayer exchange) are coupled ferromagnetically parallel to the c axis, while the moments in an adjacent plane (interlayer exchange) are coupled antiferromagnetically. In the case of $CeMn_2Ge_2$, the intralayer exchange is antiferromagnetic, while the interlayer exchange is responsible for the transition from a commensurate antiferromagnetic ordering to an incommensurate conical structure with a ferromagnetic component along the c axis and a helical component in the ab plane. Temperature dependence of the quadrupole frequency ν_Q, plotted in Fig. 2 below the Néel temperature, shows a discontinuity at 320 K. Since there is no evidence of a crystal structure change at this temperature, sudden drop in the EFG at ^{111}Cd at Mn atom site must be associated with the change of the spin structure of Mn sublattice from an antiferromagnetic to ferromagnetic alignment. A similar discontinuity in the EFG has been observed in the Mössbauer experiment.[4] Neutron-diffraction measurements[5] attributed the observed magnetic transition at 318 K to the spin reorientation of Mn atoms from antiferromagnetic to a ferromagnetic alignment. As the measured exponent β was found to be almost the same for both compounds we conclude that the nature of the antiferromagnetic order is similar in $CeMn_2Ge_2$ and $CeMn_2Si_2$. Since ^{111}Cd probe is nonmagnetic (sp-electron element), it only probes the magnetic interaction from the neighboring Mn atoms and the magnetic hyperfine field can be seen as a measure of the strength of Mn-Mn interaction. Apparently this interaction seems to be much stronger in $CeMn_2Ge_2$ than in $CeMn_2Si_2$ and could provoke a spin reorientation leading to a ferromagnetic phase transition observed in $CeMn_2Ge_2$ at lower temperature.

Departure of the temperature dependence of the hyperfine frequency for the ^{140}Ce probe in the case of $CeMn_2Ge_2$ from that of the bulk magnetization of the sample, as can be seen in Fig. 6 was already observed in some magnetic systems. The NMR frequency of ^{55}Mn in a dilute ferromagnetic FeMn alloy was experimentally shown to decrease more rapidly with temperature[11] than the magnetization of Fe host and this behavior was explained by Jaccarino, Walker, and Wertheim[12] by means of a very simple approach in which the Mn moments are believed to be localized and their magnetization is induced by the iron host. Thiel, Gerdau, and Böttcher,[13] who measured the MHF at ^{140}Ce probe nuclei in some rare-earth elements, explained their unusual temperature dependence as resulting from a mixed (3^+ and 4^+) valence in Ce probe atoms. They based their interpretation on the fact that the MHF extrapolated to $T=0$ K was found to be much lower than the magnetic field of the free Ce^{3+} ion, $B_{4f}(3^+)=183$ T.[14] This interpretation was, however, criticized by Wäckelgard *et al.*[15] who showed that the crystalline electric field, which was neglected by Thiel *et al.*, can reduce the free ion hyperfine field of Ce^{3+} in the host. Unlike the previous experiments, in the present work the ^{140}Ce probe atom is not an impurity, but one of the constituent elements of the compound itself which is an important fact as the Ce magnetism and charge in such cases can be investigated by macroscopic methods. Although the extrapolated 0 K value of the MHF of ^{140}Ce in $CeMn_2Ge_2$, $B_{hf}=39$ T, is much smaller than the free ion hyperfine field for Ce^{3+}, we can disregard the mixed valence effect in this compound. The valence of Ce ion in Ce Mn_2Si_2 and $CeMn_2Ge_2$ was experimentally measured and the results[16,17] showed an instability of Ce valence for $CeMn_2Si_2$ with a intermediate valence of 3.12 and a stable Ce^{3+} state for $CeMn_2Ge_2$. Furthermore, neutron-diffraction measurements showed no ordering of the Ce moments in either compounds.

As no ordering of the Ce moments was observed in $CeMn_2Ge_2$, we are led to believe that the additional magnetic interaction observed at the Ce sites of this compound below around 120 K, could only appear as a result of the polarization of Ce ion spin moment induced by the magnetic field from the Mn moments. As the temperature behavior of magnetic hyperfine field for ^{111}Cd at Mn sites in $CeMn_2Ge_2$ follows the Brillouin function for temperatures below 320 K (see Fig. 5), we conclude that the Ce atoms polarization does not affect the magnetic coupling among Mn spins, that is, there is no induction of spin polarization of Mn atoms from the Ce atoms. This fact provides a strong indication that the polarization of the Ce atoms by the magnetic field of Mn indeed occurs. Moreover, a first-principles density-functional

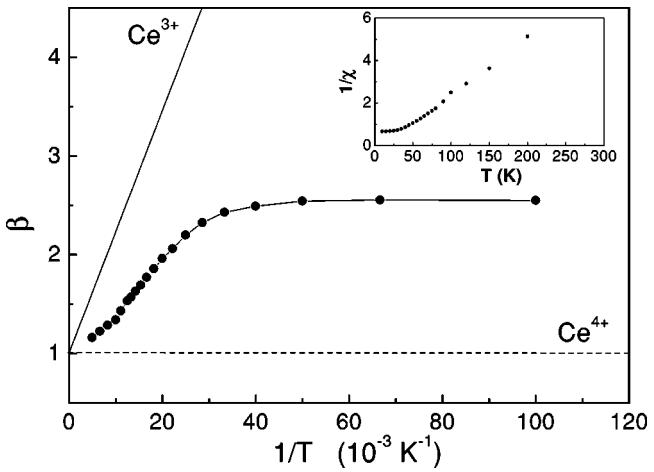

FIG. 7. The local paramagnetic enhancement factor β as a function of the inverse of the temperature for ^{140}Ce at Ce sites in $CeMn_2Ge_2$. The inset shows the temperature dependence of the inverse of the local susceptibility χ.

calculations of the magnetic hyperfine interactions for both $CeMn_2Si_2$ and $CeMn_2Ge_2$ compounds, which has been recently performed by our group,[18] showed that the Mn-Ce interaction [through the Mn($3d$)-Ce($5d$) hybridization] provides the mechanism of Ce spin alignment. The polarization of a paramagnetic rare earth sublattice by transition metal ions was proposed by Brabers *et al.*[19] to explain the temperature dependence of the susceptibility in $(Gd,La)Mn_2(Ge,Si)_2$ compounds. The same mechanism was used by Levin, Palewski, and Mydlarz[20] to explain the magnetoresistivity behavior of $CeMn_2(Ge_xSi_{1-x})_2$ compounds. It can therefore be considered that the paramagnetic Ce sublattice in $CeMn_2Ge_2$ is locally polarized by an external magnetic field from Mn ions, i.e., the magnetic hyperfine field B_{hf}^{Mn} at Ce sites, created by the magnetic ordering of Mn moments, polarizes the disordered Ce spins. In such a situation the effective magnetic field B_{eff}^{Ce} at Ce atoms is given by[21] $B_{eff}^{Ce}=B_{hf}^{Mn}+B_{hf}^{Ce}$, where B_{hf}^{Ce} is the magnetic hyperfine field at Ce nuclei due to the spin polarization of the $4f$ electrons. On the other hand, the polarization of the paramagnetic sublattice causes an increase in the magnetic induction so that[22] $B_{eff}^{Ce}=(1+\chi)B_{hf}^{Mn}=\beta B_{hf}^{Mn}$, where χ is the local magnetic susceptibility and β (not to be confused with the exponent β defined earlier) is the local paramagnetic enhancement factor. Combination of the expressions for B_{eff}^{Ce} gives the following expression for the paramagnetic enhancement factor:

$$\beta=1+\frac{B_{hf}^{Ce}}{B_{hf}^{Mn}}. \tag{4}$$

From the Larmor frequency ω_L, it is possible to determine the local paramagnetic enhancement factor using[22,23] $\omega_L(T)=(g_N\mu_N/\hbar)\beta B_{hf}^{Mn}$. The results of β as a function of the inverse temperature are shown in Fig. 7. The values of B_{hf}^{Mn} at different temperatures in the region $T<200$ K were estimated from the fit of a Brillouin function to the points for $T\geqslant 200$ K in Fig. 6. The solid line in the figure represents β values for $4f^1$ (Ce^{3+}) localized ions which were calculated from the expression[23,24] $\beta=1+g_J\mu_B(J+1)B(0)/3kT$, where $g_J=6/7$, $J=5/2$, and $B(0)=183$ T is the hyperfine field at 0 K. The horizontal line corresponds to $\beta=1$ and represents the non magnetic behavior for tetravalent Ce^{4+}. The inset in Fig. 7 shows the temperature dependence of the local susceptibility[24,25] $\chi(T)=N(\beta-1)g_J\mu_B J/B(0)$. It can be seen from Fig. 7 that the values of β for ^{140}Ce probes in the Ce sublattice of $CeMn_2Ge_2$ compound are smaller compared to that for Ce^{3+} free ion values.

Similar behavior of the temperature dependence of β at Ce sites, measured by TDPAC using ^{140}Ce, was also found in $CeFeGe_3$ (Ref. 25) and CeNiSn (Ref. 26) compounds, as well as in dilute Ce impurity in Y and Zr.[27] In each case the β values are smaller than those for free Ce^{3+} ion. In these situations the behavior of the temperature dependence of the local susceptibility was explained as a consequence of the Kondo behavior. The $\chi(t)$ values for $CeMn_2Ge_2$ could be reproduced by a Kondo model where the Kondo impurity problem within the Coqblin-Schrieffer model was solved numerically by using the Bethe-ansatz formalism.[28] In this model the behavior of the Ce ions is characterized by the zero temperature local susceptibility $\chi(0)=\nu(\nu^2-1)\mu^2/24\pi k_B T_0$ where T_0 is the characteristic scaling temperature related to the Kondo temperature[29] $T_K=0.677T_0$. Using the results from the calculations of Brickers, Cox, and Wilkins,[29] the best fit to the β values in $CeMn_2Ge_2$ yielded $T_0=27$ K, which corresponds to $T_K=18$ K. This value agrees with the expectation from the measurement of the temperature dependence of resistivity[17,20] for $CeMn_2Ge_2$ compound at zero field.

V. CONCLUSION

The PAC technique was used to investigate the hyperfine fields in $CeMn_2Ge_2$ and $CeMn_2Si_2$ intermetallic compounds by using $^{111}In\rightarrow{}^{111}Cd$ and $^{140}La\rightarrow{}^{140}Ce$ nuclear probes. A fraction of the ^{111}Cd probe nuclei were found to substitute Mn sites in both compounds. The ^{140}Ce probe was used to investigate the magnetic hyperfine fields at Ce sites. Extensive PAC measurements below the Néel temperatures have revealed important information on the magnetic properties of both compounds. The temperature dependence of the MHF at ^{111}Cd probe in $CeMn_2Si_2$ shows a transition from paramagnetic to antiferromagnetic ordering at 379 K and a standard Curie-Weiss behavior below this temperature. For $CeMn_2Ge_2$ the measurement of MHF at ^{111}Cd probe revealed a paramagnetic to antiferromagnetic phase transition at 408 K and a second transition to ferromagnetic order below 320 K. Temperature dependence of the electric-field gradient as well as the MHF in the case of $CeMn_2Ge_2$ showed sharp discontinuity at 320 K. The spin reorientation of Mn atoms is believed to be responsible for the magnetic phase transition observed at 320 K. No MHF was observed at Ce in $CeMn_2Si_2$, in the temperature range from 400 K to 10 K, and in $CeMn_2Ge_2$ in the temperature range from 408 K to 320 K, measured with ^{140}Ce probe. This fact is associated with the

symmetry of the spin-up and spin-down arrangement of the Mn superlattice around the Ce site in the antiferromagnetic phase which causes the cancellation of MHF. Between 320 K and 150 K, the MHF at Ce site in $CeMn_2Ge_2$ follows the regular behavior expected for the ferromagnetic ordering of Mn moments, however for temperatures lower than 150 K the MHF values deviate from the standard Brillouin curve and increase sharply. This behavior is explained as a local spin polarization of the Ce ions and analyzed in terms of local paramagnetic enhancement factor β at ^{140}Ce sites. The results for β values were parametrized by a Kondo model which yielded a Kondo temperature of $T_K = 18$ K.

ACKNOWLEDGMENTS

Partial financial support for this research was provided by the Fundação de Amparo para Pesquisa do Estado de São Paulo (FAPESP). M.V.L. thankfully acknowledges the financial support provided by FAPESP. We also wish to thank Dr. Jose A. H. Coaquira from IFUSP for his help in the magnetization measurements.

*Electronic address: carbonar@ipen.br
†On leave from Institute of Nuclear Sciences "Vinča," P.O. Box 522, 11001 Belgrade, Yugoslavia.

[1] F. Steglich, J. Aarts, C.D. Bredl, W. Lieke, D. Meshede, W. Franz, and H. Schäfer, Phys. Rev. Lett. **43**, 1892 (1979).
[2] K.S.V.L. Narasimhan, V.U.S. Rao, R.L. Bergner, and W.E. Wallace, J. Appl. Phys. **46**, 4957 (1975).
[3] S. Siek, A. Szytula, and J. Leciejewicz, Phys. Status Solidi **46**, K101 (1978).
[4] I. Nowik, Y. Levi, I. Felner, and E.R. Bauminger, J. Magn. Magn. Mater. **147**, 373 (1995).
[5] J.A. Fernandez-Baca, P. Hill, B.C. Chakoumakos, and N. Ali, J. Appl. Phys. **79**, 5398 (1996).
[6] R. Welter, G. Venturini, E. Ressouche, and B. Malaman, J. Alloys Compd. **218**, 204 (1995).
[7] A.W. Carbonari, J. Mestnik-Filho, R.N. Saxena, R. Dogra, and J.A.H. Coaquira, Hyperfine Interact. **136/137**, 345 (2001).
[8] M.V. Lalic and J. Mestnik-Filho (private communication).
[9] K. Królas and B. Wodniecka, H. Niewodniczanski Institute of Nuclear Physics, Kraków, Poland, Report No. 1644/OS-1993 (unpublished).
[10] A.W. Carbonari, J. Mestnik-Filho, R.N. Saxena, and H. Saitovitch, Hyperfine Interact. **133**, 77 (2001).
[11] Y. Koi, A. Tsujimura, and T. Hihara, J. Phys. Soc. Jpn. **19**, 1493 (1964).
[12] V. Jaccarino, L.R. Walker, and G.K. Wertheim, Phys. Rev. Lett. **13**, 752 (1964).
[13] T.A. Thiel, E. Gerdau, and M. Böttcher, Hyperfine Interact. **9**, 459 (1981).
[14] B. Bleany, in *Magnetic Properties of Rare Earth Metals*, edited by R.J. Elliot (Plenum, New York, 1972), p. 383.
[15] E. Wäckelgard, E. Karlsson, B. Lindgren, A. Mayer, and Z. Hrynkiewicz, Hyperfine Interact. **51**, 853 (1989).
[16] C. Ammarguellat, M. Escorne, A. Mauger, E. Beaurepaire, M.F. Ravet, G. Krill, F. Lapierre, P. Haen, and C. Godrt, Phys. Status Solidi **143**, 159 (1987).
[17] G. Liang and M. Croft, Phys. Rev. B **40**, 361 (1989).
[18] M.V. Lalic, J. Mestnik-Filho, A.W. Carbonari, and R.N. Saxena (unpublished).
[19] J.H.V.J. Brabers, C.H. de Groot, K.H.J. Buschow, and F.R. de Boer, J. Magn. Magn. Mater. **157-158**, 639 (1996).
[20] E.M. Levin, T. Palewski, and T. Mydlarz, J. Alloys Compd. **262-263**, 215 (1997).
[21] D.A. Shirley, S.S. Rosemblum, and E. Matthias, Phys. Rev. **170**, 363 (1968).
[22] C. Günther and I. Lindgren, in *Perturbed Angular Correlations*, edited by E. Karlsoon, E. Matthias, and K. Siegbahn (North-Holland, Amsteram, 1964), p. 357.
[23] H.J. Barth, G. Netz, K. Nishiyama, and D. Riegel, Phys. Rev. Lett. **45**, 1015 (1980).
[24] H.H. Bertchat, H.E. Mankhe, E. Dafni, F.D. Davidovsky, and M. Haas, Phys. Lett. A **101**, 507 (1984).
[25] A.A. Tulapurkar, S.N. Mishra, and E.V. Sampathkumaran, Hyperfine Interact. **120-121**, 199 (1999).
[26] V.V. Krishnamurthy, A.A. Tulapurkar, S.N. Mishra, S.K. Malik, D.T. Adroja, and B.D. Rainford, Physica B **223-224**, 262 (1996).
[27] V.V. Krishnamurthy, S.N. Mishra, M.R. Press, and S.H. Devare, Phys. Rev. Lett. **74**, 1661 (1995).
[28] V.T. Rajan, Phys. Rev. Lett. **51**, 308 (1983).
[29] N.E. Brickers, D.L. Cox, and J.W. Wilkins, J. Magn. Magn. Mater. **47-48**, 335 (1985).